Chapter 3
Solubility of Hydroxyapatite as a Function of Solution Composition (Experiment and Modeling)

George Kuranov, Konstantin Mikhelson and Alexandra Puzyk

Abstract Solubility of hydroxyapatite in aqueous solutions and artificial blood serum was studied at 37 °C. The obtained results demonstrate non-monotonous changes of the concentration of calcium ions in solution over time: the respective curves contain a maximum. This may be evidence in favor that dissolution of hydroxyapatite is an incongruent process. It was shown that equilibrium can be achieved in three weeks. The logarithm of activity of calcium ions exhibits a direct relation on the pH. Results of the determination of the chemical composition of solid phase obtained by XPS, EDX and ICP-OES methods confirm the incongruent nature of hydroxyapatite dissolution. In this study, we have performed a modeling of the chemical and phase equilibria in solution that served as a prototype of the blood serum with application to calcification of tissues. The concentrations of molecular–ionic forms containing calcium and hydrogen cations and phosphate anions were calculated, and the nonideality of the solutions was accounted for by the Debye–Hückel theory. The calculated degrees of salt supersaturation of different phosphates, which tend to crystallize in blood serum, demonstrate that hydroxyapatite is the most supersaturated phosphate at any values of calcium and phosphorus overall concentrations.

Keywords Hydroxyapatite solubility · Aqueous solutions · Artificial blood serum

3.1 Introduction

Hydroxyapatite (HAP) is the main mineral component of teeth, bones and one of the most common minerals in pathologic masses in human body. The solubility of hydroxyapatite has been the subject of extensive studies for several decades (Dorozhkin 2017a). Initially, the interest in this topic was caused by the need for study of the impact of external factors on dental enamel, and for the development of dental materials and means for the enamel protection. For this reason the solubility

G. Kuranov (✉) · K. Mikhelson · A. Puzyk
Institute of Chemistry, Saint Petersburg State University, Universitetsky Av., 26, Saint Petersburg 198504, Russian Federation
e-mail: g_kuranov@mail.ru

of hydroxyapatite was studied under acidic conditions. Biocompatibility of hydroxyapatite allows using this mineral as a material for various artificial implants, and a huge number of works devoted to this issue has been published in recent years (Dorozhkin 2017b). The phenomena of calcification of soft tissues also attract a lot of attention. To date, many works on the solubility of hydroxyapatite in water were published, but the reported data poorly fit together. Some literature experimental data on hydroxyapatite solubility in aqueous solutions at different pH are presented in Fig. 3.1.

It was even concluded (Levinskas and Neuman 1955) that it is impossible to determine the HAP solubility product constant. Based on the analysis of existing data on the solubility of hydroxyapatite in water, the authors of the review (Pan and Darvell 2009) concluded that it is necessary to obtain new reliable data.

One of the reasons for the discrepancy between experimental data is called incongruence of the dissolution process. It is assumed that chemical reactions take place on the surface of hydroxyapatite during the dissolution process. However, there is no reliable information about chemical transformations occurring in the system. Incongruent solubility can be attributed to differences in the rate of formation and dissolution of an intermediate solid phase (Kaufman and Kleinberg 1979). In this way, it cannot be said with confidence what solid substance (i.e., in contact with the solution) is relevant to the equilibrium. In fact, the second phase formed on hydroxyapatite may have a different composition. For example, octacalcium phosphate has been found to form on the surface of a hydroxyapatite seed in a supersaturated calcium phosphate solution (Pan and Darvell 2009). Eight dissolution models for
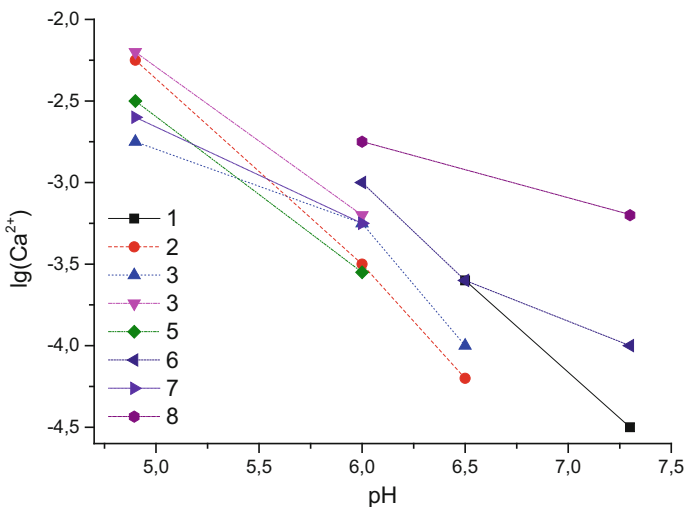

Fig. 3.1 Experimental data on hydroxyapatite solubility in aqueous solutions at different pH from literature sources: (1) Rootare et al. (1962), (2) Wier et al. (1971), (3) Avnimele et al. (1973), (4) Chuong (1973), (5) McDowell et al. (1977), (6) Bell et al. (1978), (7) Verbeeck et al. (1980), (8) Mahapatra et al. (1982)

hydroxyapatite are considered in the review (Dorozhkin 2002), but none of these is free of drawbacks.

Difficulties of the study of hydroxyapatite solubility are caused by long duration of the setting of chemical and phase equilibria and extremely low solubility. Until now, no studies of influence of electrolyte and protein composition of body fluids on the solubility of hydroxyapatite have been carried out.

Low solubility of hydroxyapatite complicates the experimental study, because even a small sampling can shift the equilibrium in the system. In this regard, it is important to provide non-destructive analysis of the composition of a solution that is in contact with hydroxyapatite. This can be done by a direct potentiometric measurement with electrode selective to calcium ions. The use of calcium ion-selective electrode (Ca-ISE) allows for a continuous measuring the composition of the solution in time, directly in the cell, without sampling. This method has an important additional advantage: the signal of the sensor depends on the activity rather than the concentration of calcium ions in solution. Thus, the data obtained by Ca-ISE are more relevant thermodynamically than those obtained by classical "wet chemistry" or by ICP-MS or other modern methods which deliver data on total (free + complexed) calcium concentration.

The lack of reliable experimental data hampered the development of thermodynamic modeling of chemical and phase equilibria in solutions that served as a prototype of the blood serum. The problems of calculating phase equilibria in calcium phosphate systems—blood serum were discussed elsewhere (Golovanova 2018; Glinkina et al. 2004).

The main goal of the present work was to get reliable data on the solubility of hydroxyapatite as a function of the solution composition, to advance in the understanding of incongruent features of HAP dissolution, and to develop a modeling approach capable of describing chemical and phase equilibria in the systems under consideration.

3.2 Experimental

3.2.1 Ca-ISE Fabrication

Calcium ionophore I diethyl N,N′-[(4R,5R)-4,5-dimethyl-1,8-dioxo-3,6-dioxaoctamethylene]bis(12-methylaminododecanoate)] (ETH 1001), potassium tetrakis-*p*-Cl-phenylborate (KClTPB), lipophilic salt tetradodecylammonium tetrakis-*p*-Cl-phenylborate (ETH 500), solvent plasticizers 2-nitrophenyloctyl ether (oNPOE) and bis(2-ethylhexyl)sebacate (DOS), high molecular weight poly(vinyl chloride) (PVC) were Selectophore grade reagents from Fluka (Switzerland). Volatile solvents were extra pure cyclohexanone (CH) and HPLC grade tetrahydrofuran (THF) from Vekton (Russia). Inorganic salts were from Reaktiv (Russia).

Table 3.1 Membrane compositions (weight percent and molality of the components)

Component	Membrane 1	Membrane 2
ETH 1001	1.03%, 0.023 m	1.02%, 0.023 m
KClTPB	0.52%, 0.016 m	0.52%, 0.016 m
ETH 500	0	1.19%, 0.016 m
Plasticizer	oNPOE, 65.63%	DOS, 64.85%
PVC	32.82%	32.42%

All aqueous solutions were prepared with deionized (DI) water with resistivity 18.2 MΩ cm (Milli-Q Reference, Millipore, France).

The membrane cocktails were prepared by dissolving appropriate amounts of PVC and oNPOE or DOS in THF. After that, ETH 1001, KClTPB and ETH 500 were added as appropriate aliquots of stock solutions in cyclohexanone. In this way, weighing of small amounts was avoided, ensuring high accuracy of the membrane composition. To obtain the membranes, the cocktails were stirred for 30 min using roller-mixer Selecta Movil Rod (Spain) and then cast on glass Petri dishes with diameter of 70 mm. The dishes were closed with filter paper to slow down the evaporation of THF. The complete evaporation of THF and CH took 2 days, and after that master membranes with a thickness of about 0.7 mm were obtained. Two membranes, respectively with oNPOE or DOS were prepared, for the membrane compositions see Table 3.1.

The electrodes were prepared by cutting disks with a diameter of 12 mm from the master membrane and gluing them to PVC bodies with outer diameter of 12 mm and inner diameter of 8 mm. A solution of PVC in CH was used as the glue. The internal reference electrode was chlorinated silver wire in a polypropylene body. Six replicate electrodes with each membrane composition were used in this work.

Initially, the ISEs were filled with 0.01 M $CaCl_2$ and conditioned in this solution for 3 days prior to measurements. After that, zero-current EMF measurements have been performed in $CaCl_2$ solutions with Lawson EMF-16 (Lawson Labs, Inc, USA). The reference electrode was a single junction Ag/AgCl electrode in 3.5 M KCl, with a salt bridge with a limited leak of KCl. Control measurements (to check the suitability of the ISEs) were carried out at room temperature (22 ± 1 °C) from 0.1 M down to 10^{-8} M $CaCl_2$ using automatic diluter Metrohm 700 Dosino controlled by Metrohm 711 Liquino Controller.

Ca^{2+}-selective membranes based on ETH 1001 are typically plasticized with polar plasticizer oNPOE because high polarity favors selectivity to divalent ions over monovalent (Bakker et al. 1997; Mikhelson 2013). However, high polarity also makes membranes prone to sorption of proteins which deteriorates the ISE response. This is why we also used DOS as plasticizer. It is known that the selectivity can be improved by adding background electrolyte: a lipophilic salt like ETH 500 (Nägele et al. 1998). Furthermore, it was shown that Ca-ISEs with low-polar membranes containing ETH 1001 and also ETH 500 show the same selectivity as those plasticized with oNPOE (Mikhelson et al. 2001; Vázquez et al. 2001).

In contact with pure $CaCl_2$ solutions, both kinds of ISEs: containing oNPOE or DOS as plasticizers, showed linear response with the slope of 29.8 mV/log(a_{Ca}) from

Table 3.2 Composition of MABS (mmol/l)

Na$^+$	K$^+$	Mg^{2+}	Cl$^-$	HCO$_3^-$	HPO$_4^{2-}$	H$_2$PO$_4^-$	C$_6$H$_{12}$O$_6$	(NH$_2$)$_2$CO	HEPES
135.5	5	0.5	109	27	2	0.5	5.5	5.5	80 g/l

0.1 to 10^{-5} M CaCl$_2$ with the detection limit of 10^{-6} M CaCl$_2$. However, in contact with model solutions containing glucose and urea ISEs with oNPOE as plasticizer did not show stable results, so we did not use these ISEs in further studies. The behavior of ISEs plasticized with DOS appeared more promising. The calibrations were stable over time and did not deteriorate after contact with model solutions containing organic substances.

3.2.2   HAP Solubility Measurement Procedure

In this work we studied the solubility of HAP in aqueous solutions at pH from 5.5 to 8.0 and in a model artificial blood serum (MABS) (but without Ca^{2+} ions and proteins) at pH = 7.4.

Sigma-Aldrich NaCl (99.5%), NaHCO$_3$ (99.5%), KCl (99.0%), Na$_2$HPO$_4$ · H$_2$O (99.5%), NaH$_2$PO$_4$ (99.5%), MgCl$_2$ · 6H$_2$O (98%), C$_6$H$_{12}$O$_6$ (99.6%), (NH$_2$)$_2$CO (99.2%), CaCl$_2$ · 2H$_2$O (99%), HEPES (99.5%) and DI water were used in the preparation of stock solutions. MABS solutions were prepared by dissolving of aliquots of stock solutions of the respective components in DI water. The composition of MABS solutions is presented in Table 3.2. The final pH value was adjusted with small aliquots of HCl or NaOH solutions at 37 °C.

Different amounts of HAP from Sigma-Aldrich (0.2 and 0.1 g) were added to glass beakers (80 ml) filled with solutions (40 ml) of the compositions studied. Closed beakers were placed in a thermostated shaker at 37.0 ± 0.5 °C. EMF measurements by Ca-ISEs were performed every two or three days until the values stabilized. It took long time (some weeks), and the MABS solutions deteriorated due to bacterial activity. To prevent that, we tried different antibacterial agents such as sodium azide, sodium benzoate, myristamidopropyldimethylbenzyl ammonium chloride, but the best results were achieved by daily irradiation with UV lamp for 15 min.

3.2.3   EMF Measurements

Before measurements in samples, ISEs were always calibrated either in aqueous CaCl$_2$: to study solubility of HAP in water, or in MABS solutions containing known amounts of CaCl$_2$: to study HAP solubility in MABS. Calibrations were performed within the range of Ca^{2+} concentration from 10^{-5} to 10^{-3} M. Model solutions containing glucose and urea did not last. Therefore, fresh calibration solutions were
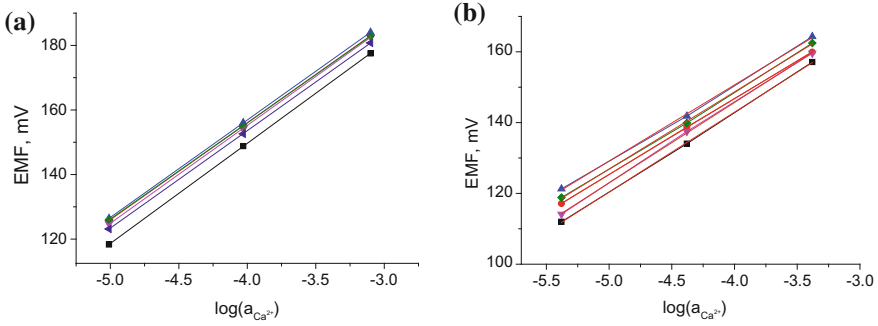
Fig. 3.2 Calibration plots of the ISEs in aqueous (**a**) and model solutions (**b**)

prepared on daily basis by dissolving of aliquots of stock solutions of the respective components in DI water.

Activities of Ca^{2+} ion in solutions were calculated according to the Davis' equation (3rd approximation of the Debye-Hückel theory):

$$\log \gamma_I = -\frac{0.512 z_I^2 \sqrt{J}}{1 + a_{Kiel} \cdot 0.328 \sqrt{J}} + 0.1 z_I J$$

Here γ_I is the ion activity coefficient, z_I is the ion charge number, J is the solution ionic strength, and a_{Kiel} is the Kielland parameter (6 for Ca^{2+}) (Dvorak et al. 1975).

Examples of the calibration results of the ISEs in aqueous and model solutions are presented in Fig. 3.2.

Preliminary measurements revealed rather low concentrations of ionized calcium in model solutions.

Therefore, to reduce the transmembrane fluxes of $CaCl_2$ co-extracted from the internal solution, the ISEs were re-filled with 10^{-3} M $CaCl_2$ and stored in the same solution in between the experiments.

3.3   Results of the Measurements

The results of the measurements reproduced several times demonstrate that the concentration of calcium ions in solution non-monotonously changes over time: the respective curves contain a maximum. The height of the maximum depends on the initial amounts of HAP (Fig. 3.3).

It took about 30 days for the equilibrium to establish, and only after that calcium ion activity becomes equal in all solutions with the same pH regardless of initial amounts of HAP.

Fig. 3.3 Dependence of Ca^{2+} ion activity on time and on initial amounts of HAP in aqueous solutions (average data for 6 ISEs)
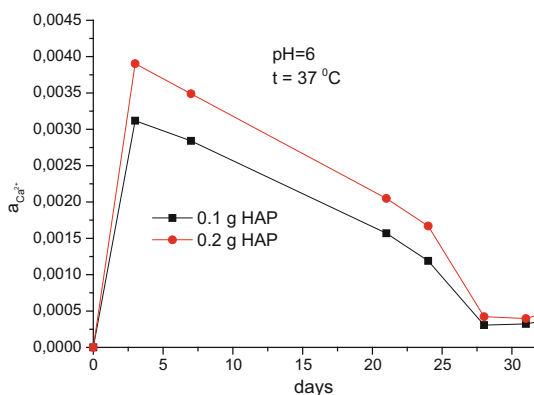
Averaged data for 6 ISEs in three parallel experiments (18 independent measurements for solution of one composition) demonstrate a linear correlation between $\log(a_{Ca})$ and the pH (Fig. 3.4).

The HAP solubility in MABS solutions has the same dynamics, but the value of solubility is lower (Fig. 3.5).

We interpret the non-monotonous change of the activity of calcium ions over time as evidence in favor of incongruent dissolution of HAP. This is in line with data reported elsewhere. Apparently, some chemical reactions occur on the surface of HAP during its dissolution. Therefore, we made some studies of the solid phase.

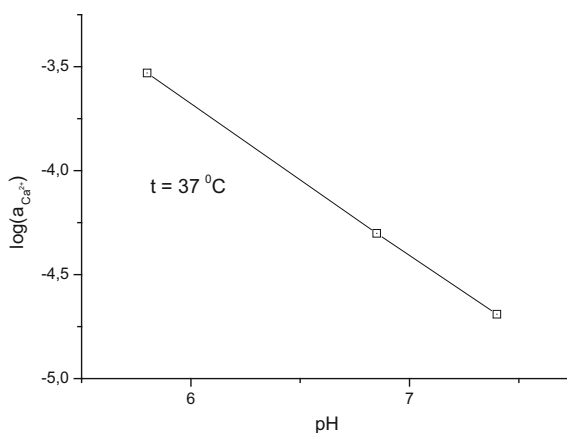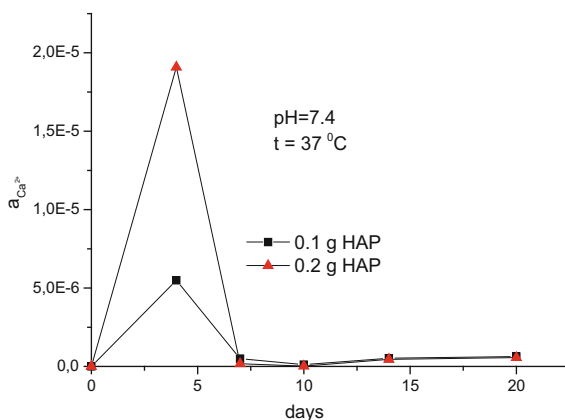**Fig. 3.4** The correlation between calcium ion activity and the pH in aqueous solutions

Fig. 3.5 Dependence of
activity of Ca^{2+} in MABS
solutions on time and on
initial amounts of HAP
(average data for 6 ISEs)

3.4 Study of Solid Phase

X-Ray photoelectron spectroscopy (XPS), energy-dispersive X-ray microanalysis
(EDX) and inductive coupled plasma optical emission spectroscopy (ICP-OES) were
used for the determination of the chemical composition of solid phase. XPS is the
surface method; depth of the electron emission is about several nanometers from the
surface. ICP-OES is used for the estimation of the total composition. EDX can be
considered as intermediate analysis with the depth of the electron emission about
several micrometers. Using all three methods simultaneously allows obtaining data
of the element distribution over the volume of a solid sample.

3.4.1 Sample Preparation

Equilibrium solid phase was decanted and washed twice with ice DI water. After
centrifugation the sediment was dried at 40 °C during 24 h. We studied solid phases
which were in equilibrium with aqueous solutions at pH 5.6, 6.6 and 7.9, and the
respective samples are denoted as S5.6, S6.6 and S7.9.

3.4.2 X-Ray Photoelectron Spectroscopy

XPS study was performed at Thermo Fisher Scientific Escalab 250Xi using AlKα
(1486.6 eV) radiation. The measured binding energies were corrected referring the
energy position of C_{1s} 284.8 eV. All the data was obtained and processed using
program complex Avantage v5.9.

3.4.3 Scanning Electron Microscopy (SEM) and Energy Dispersive X-Ray (EDX) Microanalysis

Morphology of the samples was studied with scanning electron microscope Hitachi S-3400N, accelerating voltage was 20 kV. EDX analysis was carried out with Oxford X-Max 20 add-on, probe diameter 2 μm, probe current was 1 nA.

3.4.4 Inductively Coupled Plasma–Optical Emission Spectroscopy

ICP-OES study was carried out using Shimadzu ICPE-9000. Standard samples for the calibration solutions were made of multi- and mono standards MERC in 0.1 N HNO_3.

3.4.5 Results of Solid Phase Study

SEM images of samples of HAP before and after 30 days stay in water demonstrate erosion of particles; their sizes decrease over time (Fig. 3.6).

The results of the study of elemental composition of solid phase and of the initial sample of HAP are presented in Table 3.3.

As mentioned above, XPS delivers data on the composition of the sample layers in the immediate vicinity to the interface, EDX—at depths of a few micrometers, and ICP-OES—on the whole volume of the sample. This is why the difference between
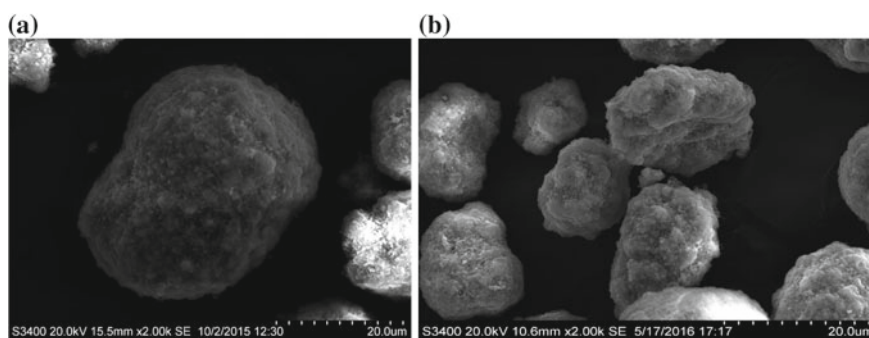

Fig. 3.6 SEM images of HAP particles before (**a**) and after (**b**) 30 days of contact with water at 37 °C

Table 3.3 Elemental composition of untreated HAP and samples by XPS, EDX, ICP-OES methods

Sample	XPS (at.%)			EDX (at.%)				ICP-OES (mol/kg)		
	O	P	Ca	Ca/P	O	P	Ca	Ca/P	P	Ca	Ca/P
S5.6	59.7	14.6	25.6	1.75	65.0	13.7	21.5	1.58	5.3	7.5	1.43
S6.6	60.5	14.9	24.6	1.65	64.5	13.7	21.8	1.57	7.0	10.2	1.45
S7.9	61.8	14.8	23.3	1.57	69.5	12.2	18.3	1.53	5.5	7.8	1.42
HAP	63.3	15.2	21.6	1.42	67.3	13.1	19.6	1.53	6.0	10.0	1.67

the numbers obtained by these three methods shows how the composition varies with the distance from the surface. The data confirm our guess about heterogeneous chemical processes occurring during dissolution of HAP. The greatest changes can be observed in the surface layer at lower pH. The relative contents of phosphorus and oxygen decrease; it may be explained by the replacement of phosphate by carbonate groups. A molar ratio of calcium to phosphorus in the samples decreases over distance from surface to bulk of the particles (Fig. 3.7). However, the results obtained by ICP-OES which refer to the total composition of a sample may be biased because the impact from the surface to the overall result increases with the decrease of the particle size.

The acidity of solutions affects primarily the composition of the surface layer (Fig. 3.8).

Figure 3.9 shows the XPS spectra of the O 1s region of S5.6 and HAP samples. Height and area of the peak of untreated HAP are bigger, besides this, one can observe an asymmetry of the pick of S5.6. The asymmetry suggests that the observed peak represents a superposition of two non-resolved peaks which refer to different binding energies. In turn, this implies that oxygen in S5.6 is involved in different chemical bonds which were not in untreated HAP.
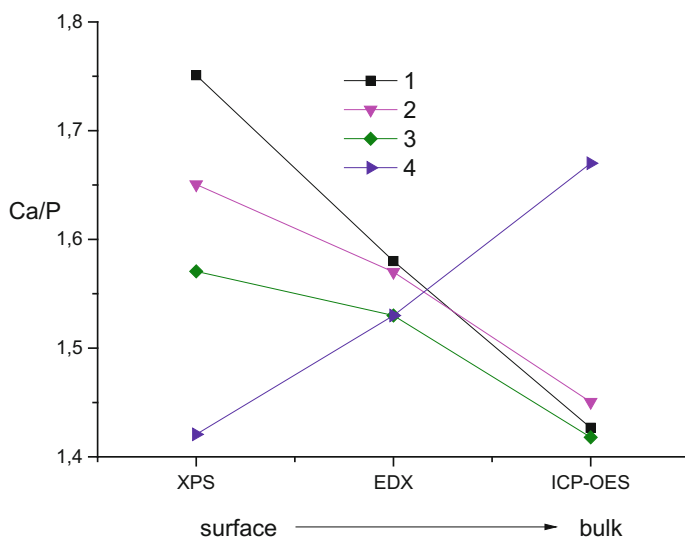

Fig. 3.7 Qualitative change profile of Ca/P in the samples: (1) S5.6, (2) S6.6, (3) S7.9, (4) HAP
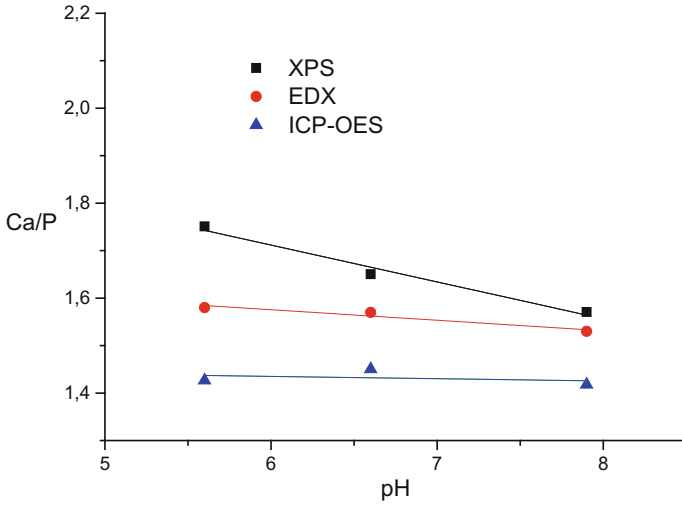
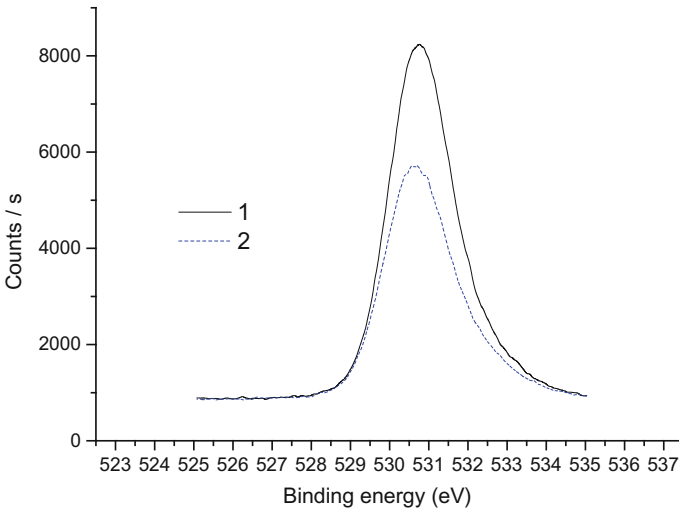**Fig. 3.8** Dependence of Ca/P on the pH of equilibrium solutions

Fig. 3.9 XPS spectra of the O 1s region of HAP (1) and S5.6 (2)

3.5 Modeling

In earlier models, organic components and ions, which do not participate in calcification of the tissues, were not taken into account, with the exception of sodium and chloride ions. Their role was assumed to be confined to their influence on the degree

of nonideality of the solutions due to electrostatic ionic interactions described by the ionic strength of the solution.

We have considered the full set of the chemical equilibria taking into account the dissociation of water and of phosphoric acid, as well as formation of both neutral and charged calcium phosphates. The equilibrium constants were written in the thermodynamic form:

$H^+ + OH^- \leftrightarrow H_2O$	$K_W = \gamma_{H^+} * C_{H^+} * \gamma_{OH^-} * C_{OH^-}$	(3.1)
$H^+ + PO_4^{3-} \leftrightarrow HPO_4^{2-}$	$K_2 = \dfrac{\gamma_{HPO_4^{2-}} * C_{HPO_4^{2-}}}{\gamma_{H^+} * C_{H^+} * \gamma_{PO_4^{3-}} * C_{PO_4^{3-}}}$	(3.2)
$H^+ + HPO_4^{2-} \leftrightarrow H_2PO_4^-$	$K_3 = \dfrac{\gamma_{H_2PO_4^-} * C_{H_2PO_4^-}}{\gamma_{H^+} * C_{H^+} * \gamma_{H_2PO_4^-} * C_{H_2PO_4^-}}$	(3.3)
$H^+ + H_2PO_4^- \leftrightarrow H_3PO_4$	$K_4 = \dfrac{\gamma_{H_3PO_4} * C_{H_3PO_4}}{\gamma_{H^+} * C_{H^+} * \gamma_{H_2PO_4^-} * C_{H_2PO_4^-}}$	(3.4)
$Ca^{2+} + H_2PO_4^- \leftrightarrow CaH_2PO_4^+$	$K_6 = \dfrac{\gamma_{CaH_2PO_4^+} * C_{CaH_2PO_4^+}}{\gamma_{Ca^{2+}} * C_{Ca^{2+}} * \gamma_{H_2PO_4^-} * C_{H_2PO_4^-}}$	(3.5)
$Ca^{2+} + H_2PO_4^- \leftrightarrow CaH_2PO_4^+$	$K_6 = \dfrac{\gamma_{CaH_2PO_4^+} * C_{CaH_2PO_4^+}}{\gamma_{Ca^{2+}} * C_{Ca^{2+}} * \gamma_{H_2PO_4^-} * C_{H_2PO_4^-}}$	(3.6)
$Ca^{2+} + OH^- \leftrightarrow CaOH^+$	$K_7 = \dfrac{\gamma_{CaOH^+} * C_{CaOH^+}}{\gamma_{Ca^{2+}} * C_{Ca^{2+}} * \gamma_{OH^-} * C_{OH^-}}$	(3.7)

C_i and γ_i are the molarity and activity coefficient of species i. For the neutral (molecular) species the activity coefficients were assumed to be unity and for the charged particles they were calculated by the Debye–Hückel equation.

Material balances of calcium and phosphorus are defined by Eqs. (3.8) and (3.9):

$$\left[Ca^{2+}\right] + [CaHPO_4] + \left[CaH_2PO_4^+\right] + \left[CaOH^+\right] = Ca^0 \qquad (3.8)$$

$$\left[PO_4^{3-}\right] + \left[HPO_4^{2-}\right] + \left[H_2PO_4^-\right] + [CaHPO_4] + \left[CaH_2PO_4^+\right] + [H_3PO_4] = P^0 \qquad (3.9)$$

where Ca^0 and P^0 are the overall concentrations of calcium and phosphorus in all forms that contain them.

The acidity of solution is defined by Eq. (3.10):

$$pH = -\lg(\gamma_{H^+} * C_{H^+}) \qquad (3.10)$$

So we have a set of ten nonlinear equations for calculation of the concentrations of 10 ionic and molecular species at given values of overall concentrations Ca^0 and P^0, pH and concentrations of sodium and chloride ions (140 mM). Thermodynamic equilibrium constants (Eqs. (3.1)–(3.7)) are known for T = 298 K (Sillen and Martell 1964).

The concentrations of molecular and ionic forms in the range of overall concentrations Ca^0 and from 0.5 to 1.5 mM and at the solution pH of 3.5–7.5 were calculated. An example of the calculated mole fractions of species at $Ca^0 = P^0 = 1$ mM is presented in Fig. 3.10.

The particular kinds of calcium phosphates which are the most important for the description of calcification of soft tissues (and therefore are of special interest) are presented in Table 3.4, together with their solubility products (Hay et al. 1982; Eidelman et al. 1987).

The calculated equilibrium concentrations of species and their activity coefficients were used to calculate the thermodynamic analogues of solubility products K'_{sp}, for example, for $Ca_3(PO_4)_2$:

$$K'_S = C^3_{Ca^{2+}} * \gamma^3_{Ca^{2+}} * C^2_{PO_4^{3-}} * \gamma^2_{PO_4^{3-}}$$
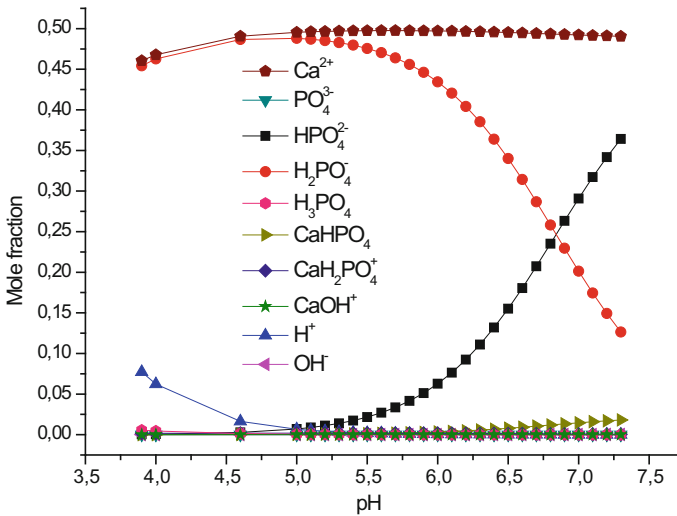

Fig. 3.10 Dependence of mole fraction of species on the pH

Table 3.4 Calcium phosphates under consideration and their solubility products (K_{sp}) (Sillen and Martell 1964)

Calcium phosphate	Formula	K_{sp}
Calcium hydrophosphate dihydrate (CHPD)	$CaHPO_4 * 2H_2O$	2.56×10^{-7}
Calcium orthophosphate (CP)	$Ca_3(PO_4)_2$	1.15×10^{-29}
Octacalcium phosphate (OCP)	$Ca_4H(PO_4)_3 * 2H_2O^a$	1.03×10^{-47}
Hydroxyapatite (HAP)	$Ca_5(PO_4)_3OH^a$	3.37×10^{-58}

[a]To simplify the calculations we used here reduced formulas of substances

The calculated values of K'_{sp} were compared with solubility products K_{sp} of the phosphates under consideration (Table 3.4). The comparison of the calculated values of K'_{sp} with the solubility products K_{sp} in solutions with different overall concentrations Ca^0 and P^0 (in all 9 compositions) at pH = 7.4 is presented in Table 3.5.

If a condition $K'_{sp} > K_{sp}$ is met for some phosphate it means that the solution is supersaturated with respect to its thermodynamically equilibrium state, and, therefore, this salt is prone to precipitation. For any values of Ca^0 and P^0 the calculated solubility product analogs for *CHPD* do not exceed the value K_{sp} and so this phosphate does not participate in the calcification of soft tissues. In the case of hydroxyapatite, all calculated values K'_{sp} are in orders of magnitude higher than the tabular data of the solubility product. Therefore from the thermodynamic point of view precipitation of hydroxyapatite plays the main role in the calcification of soft tissues.

The solution composition and the possibility of its supersaturation may conveniently be displayed graphically. The values of $\log([Ca^{2+}][OH^-]^2)$ are plotted as abscissas and the values of $\log([H^+]^3[PO_3^-])$ as ordinates. The domain of states that are supersaturated with respect to certain phosphate is above the straight line corresponding to the equation (Glinkina et al. 2004):

$$\log\left(a_{H^+}^3 * a_{PO_4^{3-}}\right) = A * \log\left(a_{Ca^{2+}} * a_{OH^-}^2\right) + B \qquad (3.11)$$

where A is the molar ratio Ca/P in the corresponding calcium phosphate and B is the constant defined by the equation for corresponding calcium phosphate (Table 3.6).

The thermodynamic state of solution with different overall concentrations Ca^0 and P^0, regarding crystallization boundaries of phosphates under study is shown in Fig. 3.11.

The distance between the point which refers to the thermodynamic state of the solution and the crystallization boundary of phosphate under study is the quantitative degree of supersaturation (χ) in respect to certain phosphates. It can be calculated according the equation:

$$\chi = \frac{A * x_0 - y_0 + B}{\sqrt{A^2 + 1}} \qquad (3.12)$$

where x_0 and y_0 are coordinates of points describing the thermodynamic state of the solution in Fig. 3.10, A and B are coefficients of Eq. (3.11) (Table 3.6). Results of calculations of degrees of supersaturation are presented in Table 3.5.

Influence of overall concentrations Ca^0 and P^0 on the degree of supersaturation with respect to phosphates under study is shown in Fig. 3.12.

Positive values of χ indicate that at given overall concentrations of Ca^0 and P^0 the solution is in a state of supersaturation. At all concentrations under consideration, HAP exhibits the highest degree of supersaturation. The degrees of supersaturation of the two other supersaturated phosphates are close to each other and much lower than for HAP. It's interesting to notice that the degree of supersaturation with respect

Table 3.5 The calculated values of K'_{sp} and supersaturation degrees χ in solutions with different overall concentrations Ca^0 and P^0 at pH $= 7.4$

Ca^0 (mM)	P^0 (mM)	CHPD $K_{sp} = 2.56 * 10^{-7}$		CP $K_{sp} = 1.15 * 10^{-29}$		OCP $K_{sp} = 1.03 * 10^{-47}$		HAP $K_{sp} = 3.37 * 10^{-58}$	
		K'_{sp}	χ	K'_{sp}	χ	K'_{sp}	χ	K'_{sp}	χ
0.5	0.5	1.27×10^{-8}	-0.92	2.26×10^{-30}	0.19	1.19×10^{-50}	-0.55	9.61×10^{-54}	0.73
0.5	1	1.88×10^{-8}	-0.36	2.34×10^{-31}	0.14	4.89×10^{-51}	-0.25	2.84×10^{-53}	0.93
0.5	1.5	4.53×10^{-8}	-0.53	2.77×10^{-29}	0.11	5.25×10^{-49}	-0.23	4.03×10^{-51}	1.01
1	0.5	3.07×10^{-8}	-0.65	3.30×10^{-29}	0.13	4.24×10^{-49}	-0.24	8.48×10^{-51}	1.07
1	1	7.48×10^{-8}	-0.38	1.92×10^{-28}	0.34	6.02×10^{-48}	-0.014	1.17×10^{-50}	1.26
1	1.5	1.10×10^{-7}	-0.26	4.07×10^{-28}	0.43	1.88×10^{-47}	0.085	3.59×10^{-50}	1.34
1.5	0.5	4.49×10^{-8}	-0.53	1.06×10^{-28}	0.27	1.98×10^{-47}	-0.11	5.92×10^{-50}	1.21
1.5	1	1.10×10^{-7}	-0.26	6.15×10^{-27}	0.48	2.83×10^{-47}	0.12	8.24×10^{-50}	1.41
1.5	1.5	1.61×10^{-7}	-0.14	1.31×10^{-26}	0.57	8.84×10^{-47}	0.22	2.53×10^{-49}	1.49

Table 3.6 The coefficients of Eq. (3.11) for phosphates under consideration

Calcium phosphate	A	B
CHPD	1	$-\log\left(K_w^2 * K_{sp} * K_2^{-1}\right)$
CP	1.33	$-\log\left(K_w^8 * K_{sp}\right)^{\frac{1}{3}}$
OCP	1.5	$-\log\left(K_w^3 * K_{sp}^{\frac{1}{2}}\right)$
HAP	1.67	$-\log\left(K_w^3 * K_{sp}^{\frac{1}{3}}\right)$
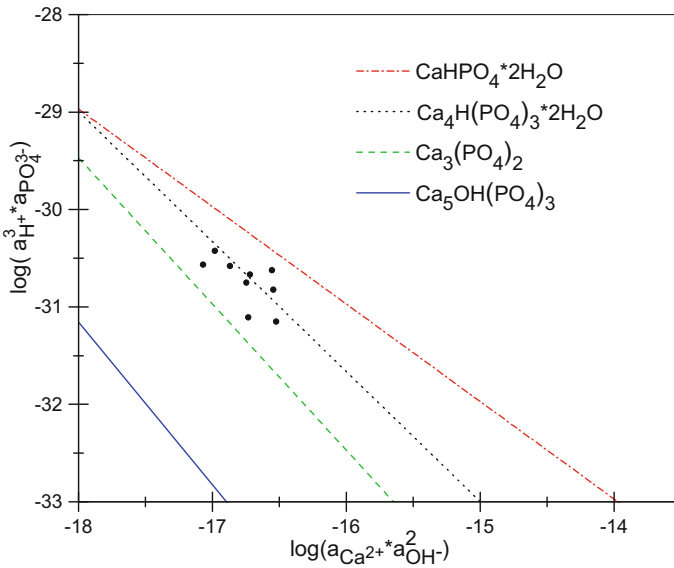
Fig. 3.11 States of the system regarding crystallization boundaries of phosphates at different overall concentrations of calcium and phosphorus at pH = 7.4

to CP is higher than that for OCP although according the values of solubility products (Table 3.4) OSP is less soluble form of calcium phosphate than CP.

It is known that the phenomena of spontaneous homogeneous and heterogeneous crystallization can be caused by various thermodynamic and kinetic factors. But the approach developed in this work allows us to give a quantitative characterization of one of the most important factors—the degree of supersaturation.
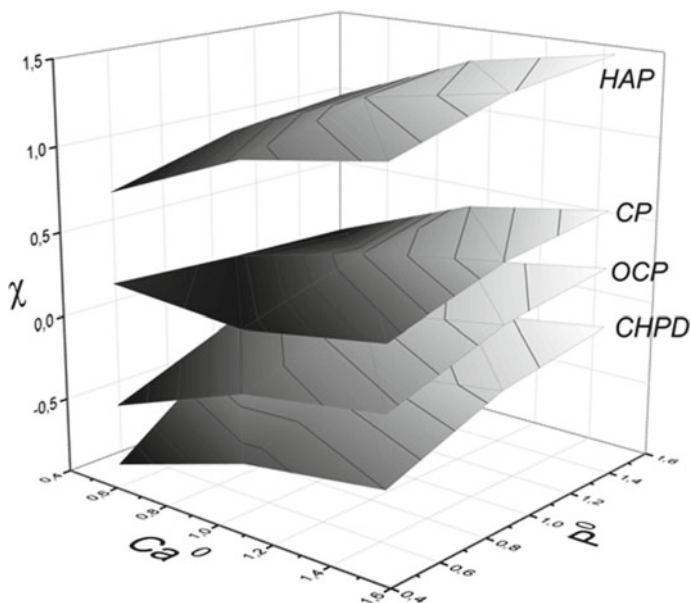
Fig. 3.12 Dependence of a degree of supersaturation on overall concentrations Ca^0 and P^0 at pH $= 7.4$

3.6 Conclusions

The obtained experimental data demonstrate that the concentration of calcium ions in HAP solutions non-monotonously changes over time. This may suggest that dissolution of hydroxyapatite is an incongruent process. The logarithm of calcium ion activity linearly correlates with the pH: activity of Ca^{2+} decreases with the pH. In principle, this is an expected result: solubility of calcium salts decreases in alkaline media. Results of determination of the chemical composition of solid phase obtained by XPS, EDX and ICP-OES reveal the changes which occurred during dissolution of HAP. All in all, the obtained results confirm that dissolution of hydroxyapatite is an incongruent process.

Calculations have been performed of molecular and ionic forms containing calcium and hydrogen cations, and phosphate anions in the total calcium and phosphorus concentrations range from 0.5 to 1.5 mM, and at the solution pH of 4.0–8.0. The calculated degrees of salt supersaturation of different phosphates, which tend to crystallize in blood's serum, demonstrate that HAP is the most supersaturated phosphate at any values of calcium and phosphorus concentrations.

References

Avnimele Y, Moreno EC, Brown WE (1973) Solubility and surface properties of finely divided hydroxyapatite. J Res Natl Bur Stand Sect A-Phys Chem A 77(1):149–155. https://doi.org/10.6028/jres.077A.008

Bakker E, Bühlmann P, Pretsch E (1997) Carrier-based ion-selective electrodes and bulk optodes. 1. General characteristics. Chem Rev 97(8):3083–3132. https://doi.org/10.1021/cr940394a

Bell LC, Mika H, Kruger BJ (1978) Synthetic hydroxyapatite solubility product and stoichiometry of dissolution. Arch Oral Biol 23(5):329–336. https://doi.org/10.1016/0003-9969(78)90089-4

Chuong R (2016) Experimental Study of Surface and Lattice Effects on the Solubility of Hydroxyapatite. J Dent Res 52(5):911–914

Dorozhkin SV (2002) A review on the dissolution models of calcium apatites. Prog Cryst Growth Charact Mater 44(1):45–61. https://doi.org/10.1016/s0960-8974(02)00004-9

Dorozhkin SV (2017a) Hydroxyapatite and other calcium orthophosphates: general information and history. Hydroxyapatite and other calcium orthophosphates: general information and history. Nova Science Publishers Inc., New York

Dorozhkin SV (2017b) A history of calcium orthophosphates ($CaPO_4$) and their biomedical applications. Morphologie 101(334):143–153. https://doi.org/10.1016/j.morpho.2017.05.001

Dvorak J, Koryta J, Bohackova V (1975) Elektrochemie. Academia, Praha

Eidelman N, Chow LC, Brown WE (1987) Calcium-phosphate phase-transformations in serum. Calcif Tissue Int 41(1):18–26. https://doi.org/10.1007/bf02555126

Glinkina IV, Durov VA, Mel'nitchenko GA (2004) Modelling of electrolyte mixtures with application to chemical equilibria in mixtures—prototypes of blood's plasma and calcification of soft tissues. J Mol Liq 110(1–3):63–67. https://doi.org/10.1016/s0167-7322(03)00233-2

Golovanova OA (2018) Thermodynamic modeling of poorly soluble compounds formation in biological fluid. J Therm Anal Calorim 133(2):1219–1224. https://doi.org/10.1007/s10973-018-7369-6

Hay DI, Schluckebier SK, Moreno EC (1982) Equilibrium dialysis and ultrafiltration studies of calcium and phosphate binding by human salivary proteins—implications for salivary supersaturation with respect to calcium-phosphate salts. Calcif Tissue Int 34(6):531–538. https://doi.org/10.1007/bf02411299

Kaufman HW, Kleinberg I (1979) Studies on the incongruent solubility of hydroxyapatite. Calcif Tissue Int 27(2):143–151. https://doi.org/10.1007/bf02441177

Levinskas GJ, Neuman WF (1955) The solubility of bone mineral. 1. Solubility studies of synthetic hydroxylapatite. J Phys Chem 59(2):164–168. https://doi.org/10.1021/j150524a017

Mahapatra PP, Mishra H, Chickerur NS (1982) Solubility and thermodynamic data of cadmium hydroxyapatite in aqueous media. Thermochim Acta 54(1–2):1–8. https://doi.org/10.1016/0040-6031(82)85059-4

McDowell H, Gregory TM, Brown WE (1977) Solubility of $Ca_5(PO_4)_3OH$ in system $Ca(OH)_2$–H_3PO_4–H_2O at 5, 15, 25 and 37 °C. J Res Natl Bur Stand Sect A-Phys Chem A 81(2–3):273–281. https://doi.org/10.6028/jres.081A.017

Mikhelson KN (2013) Ion-selective electrodes, vol 81. Lecture notes in chemistry. Springer, Heidelberg-New York-Dordrecht-London

Mikhelson KN, Bobacka J, Lewenstam A, Ivaska A (2001) Potentiometric performance and interfacial kinetics of neutral Ionophore based ISE membranes in interfering ion solutions before and after contact with primary ions. Electroanalysis 13(10):876–881. https://doi.org/10.1002/1521-4109(200106)13:10%3c876:aid-elan876%3e3.0.co;2-%23

Nägele M, Mi Y, Bakker E, Pretsch E (1998) Influence of lipophilic inert electrolytes on the selectivity of polymer membrane electrodes. Anal Chem 70(9):1686–1691. https://doi.org/10.1021/ac970903j

Pan HB, Darvell BW (2009) Calcium phosphate solubility: the need for re-evaluation. Cryst Growth Des 9(2):639–645

Rootare HM, Deitz VR, Carpenter FG (1962) Solubility product phenomena in hydroxyapatite-water systems. J Colloid Sci 17(3):179–206. https://doi.org/10.1016/0095-8522(62)90035-1

Sillen LG, Martell AE (eds) (1964) Stability constants of metal-ion complexes, 2nd edn. Pergamon Press, Oxford

Vázquez M, Mikhelson K, Piepponen S, Räinö J, Sillanpää M, Ivaska A, Lewenstam A, Bobacka J (2001) Determination of Na^+, K^+, Ca^{2+}, and Cl^- ions in wood pulp suspension using ion-selective electrodes. Electroanalysis 13(13):1119–1124. https://doi.org/10.1002/1521-4109(200109)13:13%3c1119:aid-elan1119%3e3.0.co;2-m

Verbeeck RMH, Thun HP, Driessens FCM (1980) Effect of dehydration of hydroxyapatite on its solubility behaviour. Z Phys Chem 119(1):79–84. https://doi.org/10.1524/zpch.1980.119.1.079

Wier DR, Chien SH, Black CA (1971) Solubility of hydroxyapatite. Soil Sci 111(2):107. https://doi.org/10.1097/00010694-197102000-00005